doi:10.1093/brain/aww148 BRAIN 2016: 139; 2516–2527 | 2516

BRAIN
A JOURNAL OF NEUROLOGY

Relative impact of amyloid-β, lacunes, and downstream imaging markers on cognitive trajectories

Hee Jin Kim,[1,2] Jin Ju Yang,[3] Hunki Kwon,[3] Changsoo Kim,[4] Jong Min Lee,[3] Phillip Chun,[5,6] Yeo Jin Kim,[1,2,7] Na-Yeon Jung,[1,2,8] Juhee Chin,[1,2] Seonwoo Kim,[9] Sook-young Woo,[9] Yearn Seong Choe,[10] Kyung-Han Lee,[10] Sung Tae Kim,[11] Jae Seung Kim,[12] Jae Hong Lee,[13] Michael W. Weiner,[14] Duk L. Na[1,2,15] and Sang Won Seo[1,2,16]

See Cohen (doi:10.1093/aww183) for a scientific commentary on this article.

Amyloid-β and cerebral small vessel disease are the two major causes of cognitive impairment in the elderly. However, the underlying mechanisms responsible for precisely how amyloid-β and cerebral small vessel disease affect cognitive impairment remain unclear. We investigated the effects of amyloid-β and lacunes on downstream imaging markers including structural network and cortical thickness, further analysing their relative impact on cognitive trajectories. We prospectively recruited a pool of 117 mild cognitive impairment patients (45 amnestic type and 72 subcortical vascular type), from which 83 patients received annual follow-up with neuropsychological tests and brain magnetic resonance imaging for 3 years, and 87 patients received a second Pittsburgh compound B positron emission tomography analysis. Structural networks based on diffusion tensor imaging and cortical thickness were analysed. We used linear mixed effect regression models to evaluate the effects of imaging markers on cognitive decline. Time-varying Pittsburgh compound B uptake was associated with temporoparietal thinning, which correlated with memory decline (verbal memory test, unstandardized $\beta = -0.79$, $P < 0.001$; visual memory test, unstandardized $\beta = -2.84$, $P = 0.009$). Time-varying lacune number was associated with the degree of frontoparietal network disruption or thinning, which further affected frontal-executive function decline (Digit span backward test, unstandardized $\beta = -0.05$, $P = 0.002$; Stroop colour test, unstandardized $\beta = -0.94$, $P = 0.008$). Of the multiple imaging markers analysed, Pittsburgh compound B uptake and the number of lacunes had the greatest association with memory decline and frontal-executive function decline, respectively: Time-varying Pittsburgh compound B uptake (standardized $\beta = -0.25$, $P = 0.010$) showed the strongest effect on visual memory test, followed by time-varying temporoparietal thickness (standardized $\beta = 0.21$, $P = 0.010$) and time-varying nodal efficiency (standardized $\beta = 0.17$, $P = 0.024$). Time-varying lacune number (standardized $\beta = -0.25$, $P = 0.014$) showed the strongest effect on time-varying digit span backward test followed by time-varying nodal efficiency (standardized $\beta = 0.17$, $P = 0.021$). Finally, time-varying lacune number ($\beta = -0.22$, $P = 0.034$) showed the strongest effect on time-varying Stroop colour test followed by time-varying frontal thickness (standardized $\beta = 0.19$, $P = 0.026$). Our multimodal imaging analyses suggest that cognitive trajectories related to amyloid-β and lacunes have distinct paths, and that amyloid-β or lacunes have greatest impact on cognitive decline. Our results provide rationale for the targeting of amyloid-β and lacunes in therapeutic strategies aimed at ameliorating cognitive decline.

1 Departments of Neurology, Samsung Medical Center, Sungkyunkwan University School of Medicine, Seoul, Korea
2 Neuroscience Center, Samsung Medical Center, Seoul, Korea
3 Department of Biomedical Engineering, Hanyang University, Seoul, Korea
4 Department of Preventive Medicine, Yonsei University College of Medicine, Seoul, Korea
5 Department of Emergency Medicine Behavioral Emergencies Research Lab, San Diego, CA, USA
6 Department of Biology, University of California San Diego, CA, USA

Received December 9, 2015. Revised April 6, 2016. Accepted May 5, 2016. Advance Access publication June 21, 2016
© The Author (2016). Published by Oxford University Press on behalf of the Guarantors of Brain. All rights reserved.
For Permissions, please email: journals.permissions@oup.com

Downloaded from https://academic.oup.com/brain/article/139/9/2516/1744564 by Hanyang Univ Lib user on 03 September 2021

7 Department of Neurology, Chuncheon Sacred Heart Hospital, Hallym University College of Medicine, Chuncheon, Korea
8 Department of Neurology, Pusan National University Hospital, Pusan National University School of Medicine and Medical Research Institute, Busan, Republic of Korea
9 Biostatistics team, Samsung Biomedical Research Institute
10 Department of Nuclear Medicine, Samsung Medical Center, Sungkyunkwan University School of Medicine, Seoul, Korea
11 Department of Radiology, Samsung Medical Center, Sungkyunkwan University School of Medicine, Seoul, Korea
12 Department of Nuclear Medicine, Asan Medical Center, University of Ulsan College of Medicine, Seoul, Korea
13 Department of Neurology, Asan Medical Center, University of Ulsan College of Medicine, Seoul, Korea
14 Center for Imaging of Neurodegenerative Diseases, University of California, San Francisco, CA, USA
15 Department of Health Sciences and Technology, SAIHST, Sungkyunkwan University, Seoul, Korea
16 Department of Clinical Research Design and Evaluation, SAIHST, Sungkyunkwan University, Seoul, Korea

Correspondence to: Sang Won Seo, MD, PhD
Department of Neurology,
Sungkyunkwan University School of Medicine,
Samsung Medical Center, 50 Ilwon-dong, Gangnam-gu,
Seoul 135-710, Republic of Korea
E-mail: sangwonseo@empal.com

Keywords: mild cognitive impairment; amyloid-β; cerebral small vessel disease; downstream imaging markers; cognitive trajectory

Abbreviations: COWAT = Controlled Oral Word Association Test; CDR-SOB = clinical dementia rating sum of boxes; CSVD = cerebral small vessel disease; MCI = mild cognitive impairment; PiB = Pittsburgh compound B; RCFT = Rey-Osterrieth Complex Figure Test; SUVR = standardized uptake value ratio; WMH = white matter hyperintensity

Introduction

Alzheimer's disease and cerebral small vessel disease (CSVD) are the two major causes of cognitive impairment in the elderly. Amnestic mild cognitive impairment (MCI) is often the result of Alzheimer's disease pathology associated with widespread brain amyloid-β burden (Petersen, 2004), while subcortical vascular MCI is more associated with frontal-executive dysfunction arising from extensive CSVD (Kim *et al.*, 2014). Recent pathological and *in vivo* amyloid PET studies have shown that many patients have concomitant amyloid-β and CSVD burden (Schneider *et al.*, 2007; Lee *et al.*, 2011*a*).

With the advent of Alzheimer's disease biomarkers, a hypothetical model of the temporal evolution of Alzheimer's disease biomarkers was recently proposed. That is, amyloid-β changes occurred earliest followed by downstream markers including network disruption, tau deposition, brain atrophy and cognitive impairments. Previous studies showed that CSVD are associated with network disruption and brain atrophy, which are further associated with cognitive impairments (Seo *et al.*, 2010, 2012; Kim *et al.*, 2015*b*, 2016). More recent cross-sectional studies from our group suggested that amyloid-β and CSVD affected downstream markers, including structural network disruption and cortical thinning in specific regions, which in turn led to impairments in their cognitive domains (Kim *et al.*, 2015*a*; Ye *et al.*, 2015). However, few studies have longitudinally investigated the relationships between amyloid-β, CSVD, and their associated brain structural changes (Lo *et al.*, 2012; Mattsson *et al.*, 2015), and to our knowledge no studies have sought to determine which imaging marker has a stronger influence on cognitive decline. Considering previous studies indicating that brain structural changes might be the final common pathway between amyloid-β/CSVD burden and cognitive impairments (Sabri *et al.*, 1999; Fein *et al.*, 2000; Mungas *et al.*, 2001; Preul *et al.*, 2005; Ewers *et al.*, 2012; Jack *et al.*, 2013), downstream imaging markers of brain structural changes triggered by amyloid-β and CSVD may have the greatest impact on cognitive trajectories. Adding further complication to the matter is the existence of several cross-sectional studies that have shown that amyloid-β and CSVD can affect cognitive impairment in the presence or absence of mediation by downstream changes (Villeneuve *et al.*, 2014; Kim *et al.*, 2015*a*; Ye *et al.*, 2015). It would therefore be reasonable to hypothesize that amyloid-β or CSVD burden itself, regardless of downstream changes, might also be the major factors affecting cognitive trajectories.

In this study, we repeatedly measured multimodal imaging markers over 3 years, including amyloid-β burden measured by Pittsburgh compound B (PiB) standardized uptake value ratios (SUVRs), CSVD burden measured by assessment of lacunes. For the downstream imaging markers triggered by amyloid-β or CSVD, we analysed structural network measured by diffusion tensor imaging-based nodal efficiency, and cortical thickness. We hypothesized that amyloid-β or CSVD changes affected the progression of downstream markers in specific regions, which in turn lead to the decline in their corresponding cognitive domains. We further hypothesized that the progression of downstream imaging markers would have greater impact on cognitive decline than amyloid-β or CSVD changes.

Downloaded from https://academic.oup.com/brain/article/139/9/2516/1744564 by Hanyang Univ Lib user on 03 September 2021

Materials and methods

Participants

We prospectively recruited 117 patients with MCI (45 with amnestic MCI and 72 with subcortical vascular MCI) between September 2008 and September 2011 at Samsung Medical Center in Seoul, Korea. Patients were diagnosed with MCI using the Petersen's criteria (Petersen *et al.*, 1999) with the following modifications, which have been previously described in detail (Seo *et al.*, 2009): (i) a subjective cognitive complaint by the patient or his/her caregiver; (ii) normal Activities of Daily Living (ADL) score determined clinically and by the instrumental ADL scale (Ku *et al.*, 2004); (iii) an objective cognitive decline below the 16th percentile [−1.0 standard deviation (SD) of age- and education-matched norms in at least one of four cognitive domains (language, visuospatial, memory or frontal-executive function] on neuropsychological tests described below (Ahn *et al.*, 2010); and (iv) absence of dementia.

Of those who met the MCI criteria, subcortical vascular MCI was further diagnosed when patients had subcortical vascular features defined as a focal neurological symptom/sign, which could include corticobulbar signs, pyramidal signs, or parkinsonism (Kim *et al.*, 2010), as well as significant ischaemia on MRI. Significant ischaemia was defined as white matter hyperintensities (WMHs) on T_2-weighted or fluid-attenuated inversion recovery (FLAIR) images that satisfied the following criteria: (i) WMH $\geqslant$ 10 mm in the periventricular white matter (caps or rim); and (ii) WMH $\geqslant$ 25 mm (maximum diameter) in the deep white matter, consistent with an extensive white matter lesion or diffusely confluent lesion. Of those who met the MCI criteria, amnestic MCI was further diagnosed when patients showed objective memory decline below the 16th percentile (−1.0 SD) of age- and education-matched norms on verbal or visual memory test as described below, and did not have significant ischaemia on MRI as described above.

Patients were evaluated by clinical interview and neurological and neuropsychological examinations as previously described (Seo *et al.*, 2007). All patients underwent laboratory tests including a complete blood count, blood chemistry, vitamin B_{12}/folate, syphilis serology, and thyroid function tests. Brain MRI confirmed the absence of structural lesions including territorial cerebral infarction, brain tumours, hippocampal sclerosis, and vascular malformation.

After a complete description of the study to the subjects, written informed consent was obtained from each patient. The Institutional Review Board of Samsung Medical Center approved the study protocol.

Neuropsychological tests

All patients were annually followed up with the Seoul Neuropsychological Screening Battery (SNSB) (Kang and Na, 2003; Ahn *et al.*, 2010). The battery contains tests for language, visuospatial function, verbal and visual memory, and frontal-executive function. Language was assessed as abnormal when the score on the Korean version of the Boston Naming Test (K-BNT) (Kim and Na, 1999) was below the 16th percentile of the norm; visuospatial function was considered abnormal when the copying score of the Rey-Osterrieth Complex Figure Test (RCFT) was below the 16th percentile of the norm; and memory function was considered abnormal when the score of 20-min delayed recall on Seoul Verbal Learning Test (SVLT) or RCFT was below the 16th percentile of the norm. Frontal executive tests were classified into three groups: motor executive function (contrasting program, Go/No-go, fist-edge-palm, alternating hand movement, alternative square and triangle, and Luria loop), Controlled Oral Word Association Test (COWAT), and Stroop Test. Abnormal frontal-executive function was operationally defined as impairment in at least two of the three groups. The norms for each of the above tests were based on assessments of 447 normal Korean participants.

In this study, to assess verbal and visual memory functions, we analysed SVLT delayed recall (range 0 to 12) and RCFT delayed recall (range 0 to 36) tests, respectively. To assess frontal-executive function, we analysed digit span backward (range 0 to 8), phonemic COWAT (range 0 to 45), and Stroop colour reading test (range 0 to 112). General cognition was assessed by clinical dementia rating sum of boxes (CDR-SOB, range 0 to 30). The Korean version of the mini-mental state examination (K-MMSE, range 0 to 30) was also performed.

MRI acquisition

We acquired standardized T_2, 3D T_1 turbo field echo images, 3D FLAIR, and DTIs from all participants at Samsung Medical Center using the same 3.0T MRI scanner (Philips 3.0 T Achieva; Philips Healthcare). The 3D T_1 turbo field echo magnetic resonance images were acquired using the following parameters: sagittal slice thickness, 1.0 mm, over contiguous slices with 50% overlap; no gap; repetition time of 9.9 ms; echo time of 4.6 ms; flip angle of 8°, and matrix size of 240 × 240 pixels, reconstructed to 480 × 480 over a field of view of 240 mm. The following parameters were used for the 3D FLAIR images: axial slice thickness of 2 mm; no gap; repetition time of 11 000ms; echo time of 125 ms; flip angle of 90°; and matrix size of 512 × 512 pixels. On whole-brain diffusion tensor-MRI examination, sets of axial diffusion-weighted, single-shot, echo-planar images were collected with the following parameters: 128 × 128 acquisition matrix, 1.72 × 1.72 × 2 mm^3 voxel size; 70 axial slices; 22 × 22 cm^2 field of view; echo time 60 ms, repetition time 7696 ms; flip angle 90°; slice gap 0 mm; b-factor of 600 s/mm^2. Diffusion-weighted images were acquired from 45 different directions using a baseline image without weighting [0,0,0]. All axial sections were acquired parallel to the anterior commissure-posterior commissure line.

Assessment of lacunes on MRI

Lacunes were defined as small lesions ($\leqslant$15 mm and $\geqslant$3 mm in diameter) with low signal on T_1-weighted images, high signal on T_2-weighted images, and a perilesional halo on 80 axial slices of FLAIR images. These criteria meet the definition of lacunes of presumed vascular origin, recently proposed by Wardlaw *et al.* (2013). Two neurologists manually counted the number of lacunes, with a kappa value of 0.78.

Downloaded from https://academic.oup.com/brain/article/139/9/2516/1744564 by Hanyang Univ Lib user on 03 September 2021

Assessment of total cerebral small vessel disease score on MRI

We rated the total MRI burden of CSVD on a scale from 0 to 4, by counting the presence of each of the four MRI features of CSVD: lacune, microbleed, perivascular space, and WMHs (Staals *et al.*, 2014).

^{11}C-PiB-PET imaging and data analysis

All patients underwent the ^{11}C-PiB-PET scans at Samsung Medical Center or Asan Medical Center with identical settings using a Discovery STe PET/CT scanner (GE Medical Systems). ^{11}C-PiB-PET scanning was performed in 3D scanning mode examining 35 slices of 4.25-mm thickness spanning the entire brain. ^{11}C-PiB was injected into an antecubital vein as a bolus with a mean dose of 420 MBq (range 259–550 MBq). CT scans were performed for attenuation correction 60 min after injection. A 30-min emission static PET scan was then initiated. The specific radioactivity of ^{11}C-PiB at the time of administration was >1500 Ci/mmol for patients and the radiochemical yield was $>35\%$. The radiochemical purity of the tracer was $>95\%$ in all PET studies.

PiB-PET images were co-registered to individual MRIs, which were normalized to a T_1-weighted MRI template. Using these parameters, MRI co-registered PiB-PET images were normalized to the MRI template. The quantitative regional values of PiB retention on the spatially normalized PiB images were obtained by an automated volume of interest analysis using the automated anatomical labelling atlas (AAL) atlas. Data processing was performed using SPM Version 5 (SPM5) within Matlab 6.5 (MathWorks, Natick, MA).

We selected 28 cortical volumes of interest from left and right hemispheres using the AAL atlas. The cerebral cortical volumes of interest that were chosen for this study consisted of the bilateral frontal, posterior cingulate gyri, parietal, lateral temporal, and occipital areas. Regional cerebral cortical uptake ratios were calculated by dividing each cortical volume of interest uptake ratio by the mean uptake of the cerebellar cortex (cerebellum crus1 and crus2). Global PiB SUVR was calculated from the volume-weighted average uptake ratio of the bilateral 28 cerebral cortical volumes of interest. We used PiB SUVR as a continuous variable representing the degree of amyloid-β burden.

Network node and edge definition

Network nodes were defined based on the AAL (Tzourio-Mazoyer *et al.*, 2002), which parcellates the cerebral cortex into 78 areas (39 regions in each hemisphere). Individual T_1-weighted images were non-linearly registered to the ICBM152 T_1 template in Montreal Neurological Institute (MNI) space (Collins *et al.*, 1994). The AAL atlas was transformed from MNI space to T_1 native space through inverse transformation with a nearest neighbour interpolation method.

We corrected distortions in DTIs caused by eddy currents and simple head motions using the FSL (FMRIB's Software Library) package diffusion toolbox in the FSL package (www.fmrib.ox.ac.uk/fsl/fdt). Diffusion tensor models were estimated, and the fractional anisotropy and mean diffusivity were calculated at each voxel. We reconstructed whole-brain white matter fibre tracts in native diffusion space for each subject using the fibre assignment of the continuous tracking algorithm (Mori *et al.*, 1999) embedded in the Diffusion Toolkit (trackvis.org) (Wang *et al.*, 2007). We terminated tracking when the angle between two consecutive orientation vectors was greater than the given threshold of 45° or when both ends of the fibres extended outside of the white matter mask generated by the tissue segmentation process (Kim *et al.*, 2013). A fibre cutoff filter was applied such that fibres shorter than 20 mm and longer than 200 mm were eliminated.

T_1-weighted images were co-registered to the b0 images using the affine registration tool from the FSL package (www.fmrib.ox.ac.uk/fsl/ flirt). Reconstructed whole-brain fibre tracts were inversely transformed into the T_1 space, and fibre tracts and AAL-based parcellated regions were located in the same space. Two nodes (regions) were considered to be structurally connected by an edge when at least the endpoints of three-fibre tracts were located in these two regions. A threshold for the number of fibre tracts was selected to reduce the risk of false-positive connections due to noise or limitations in the deterministic tractography (Kim *et al.*, 2013). The fractional anisotropy value is considered an important index to evaluate fibre integrity (Beaulieu, 2002), and in this study, the mean fractional anisotropy value along all fibres connecting pairs of regions was used to weight the edge. Finally, weighted structural networks represented by symmetric 78×78 matrices were constructed for each individual.

Network analysis

Graph theoretical analyses were performed on weighted connectivity networks using the Brain Connectivity Toolbox (www.brain-connectivity-toolbox.net) (Rubinov and Sporns, 2010). We used nodal efficiency as a nodal topological characteristic of structural network, defined using the inverse of the weighted shortest path length between a given node and all other nodes in the network (Rubinov and Sporns, 2010). This metric quantifies the importance of each node for communication within the network, and nodal efficiency was measured for each node. Decreased nodal efficiency indicates decreased integration in local regions, suggesting more disruptive structural network in these regions. Averaged values of the nodal efficiency (mean nodal efficiency) in the global cortex, frontal, and temporoparietal regions predefined in the AAL atlas were used.

Cortical thickness data analysis

T_1-weighted images were processed using the standard MNI anatomical pipeline. Further image processing tools used for the cortical thickness measurements have been described in a previous study (Kim *et al.*, 2015*a*). From this method, we obtained the mean thickness of the frontal lobe and temporoparietal lobe.

Follow-up evaluations with neuropsychological tests, MRI and PiB-PET

All the patients underwent clinical interviews, a neurological examination, neuropsychological tests, brain MRI, and PiB-PET imaging at baseline. Patients were annually evaluated for 3 years

Downloaded from https://academic.oup.com/brain/article/139/9/2516/1744564 by Hanyang Univ Lib user on 03 September 2021

through clinical interviews, neuropsychological tests and brain MRI. PiB-PET was followed in the second or third year.

Statistical analyses

Mean ± SD, and frequency (%) were presented for continuous variable and categorical variable, respectively. To obtain a wide range of values for PiB SUVR and the number of lacunes, we combined the two MCI subtypes (amnestic and subcortical vascular MCI) in the analyses, with the MCI subtype adjusted in each model.

To evaluate the relationship between time-varying PiB SUVR and time-varying lacune number over time, we used a linear mixed effect regression model and included time-varying PiB SUVR as a fixed effect along with age, gender, MCI subtype, and time interval from baseline (years). Subject was included as a random effect.

To evaluate the topography of structural network disruption (measured by nodal efficiency) or cortical thinning as a function of time-varying PiB SUVR or lacune number over time, we included these parameters as fixed effects along with other variables. Because multiple comparisons were performed for 78 nodal regions (for network analysis) and 81 924 vertices (for cortical thickness analysis), we determined an uncorrected P-value of < 0.01 to be significant.

Then, to assess the effects of multiple imaging markers on cognitive decline, we sequentially used two linear mixed effect regression models. In Model 1, we included time-varying PiB SUVR and number of lacunes over time as fixed effects, along with other variables. We also evaluated interactive effects of time-varying PiB SUVR and time-varying lacune number over time on cognitive decline. For Model 2 and 3, longitudinal measurements of either regional nodal efficiency or regional cortical thickness was added to Model 1: global cortical thickness or global nodal efficiency was added in the analysis for CDR-SOB; temporoparietal thickness or temporoparietal nodal efficiency was added in the analysis for memory decline; and frontal thickness or frontal nodal efficiency was added in the analysis for frontal-executive function decline. For the SVLT delayed recall analysis, we used a generalized linear mixed model with negative binomial distribution. For the CDR-SOB analysis, we used a mixed linear model after transforming the data into log scale (CDR-SOB + 1), as the data was not normally distributed.

Then, to evaluate the relative impact of each imaging marker on cognitive tests that were associated with two or more imaging markers, we estimated the standardized β-values after standardizing the data. We did not analyse relative impact of multimodal imaging markers on SVLT delayed recall because SVLT delayed recall score had negative binomial distribution.

Statistical analyses were conducted with SAS 9.3 (SAS Institute, Cary, NC).

Results

Subject demographics and longitudinal follow-up

Demographic information of the subjects is shown in Table 1. Of the 117 MCI patients, 97 completed the first year of follow-up, 82 completed the second year of follow-up, and 83 (70.9%) completed the third year of follow-up. A total of 87 patients underwent a secondary PiB-PET scan with a mean interval of 32.0 months.

Among 83 patients who completed 3 year follow-ups, 23 patients (27.7%) converted to dementia: 13/30 (43.3%) among amnestic MCI patients and 10/53 (18.9%) among patients with subcortical vascular MCI. After considering various factors, we found that female, amnestic MCI, higher baseline amyloid burden, lower baseline cortical thickness increased risk of dementia conversion in our MCI cohort (Table 2, Model 2).

PiB SUVR increased from 1.62 to 1.67 ($P = 0.003$) (1.86 to 1.95 in amnestic MCI, 1.47 to 1.52 in subcortical vascular MCI) over 32 months, and the number of lacunes increased from 4.5 to 5.7 ($P = 0.001$) (0.8 to 1.0 in amnestic MCI, 6.8 to 7.9 in subcortical vascular MCI) over 3 years. Cortical thickness decreased over 3 years (< 0.001) while change in nodal efficiency did not reach significance ($P = 0.212$) (Supplementary Table 1). Time-varying PiB SUVR was negatively associated with time-varying lacune number ($\beta = -1.74$, $P = 0.034$).

Topography of decreased nodal efficiency and cortical thinning associated with increased PiB SUVR and the number of lacunes

Over the 3 years, time-varying lacune number showed a negative correlation with the time-varying nodal efficiency especially in the frontal and parietal areas (Fig. 1 and Table 3), which indicates that increased number of lacunes affected more disruptive structural network in these regions. However, time-varying PiB SUVR did not show a correlation with time-varying nodal efficiency.

Time-varying PiB SUVR showed a negative correlation with time-varying cortical thickness, especially in the medial temporal and precuneus regions, whereas time-varying lacune number showed a negative correlation with time-varying cortical thickness especially in the medial/lateral frontal, lateral parietal, and parieto-occipito-temporal regions (Fig. 1).

Effects of multimodal imaging markers on cognitive decline

Over the 3-year period, time-varying PiB SUVR showed a negative correlation with time-varying cognitive function in SVLT and RCFT delayed recall, as well as CDR-SOB, while time-varying lacune number showed a negative correlation with time-varying cognitive function in digit span backward and Stroop colour reading tests (Table 4, Model 1). There was no interactive effect between time-varying PiB SUVR and time-varying lacune number on change in CDR-SOB [$\beta = 0.02$, standard error (SE) = 0.07, $P = 0.953$], SVLT delayed recall ($\beta = 0.09$, SE = 0.13, $P = 0.511$), RCFT

Downloaded from https://academic.oup.com/brain/article/139/9/2516/1744564 by Hanyang Univ Lib user on 03 September 2021

Table 1 Baseline characteristics of the participants

	Total *n* = 117	Amnestic MCI *n* = 45	Subcortical vascular MCI *n* = 72	*P*
Demographics				
Age	72.9 ± 7.3	71.1 ± 7.7	74.0 ± 6.9	0.034
Male: Female	53: 64	26: 19	27: 45	0.032
Education, yrs	10.2 ± 5.3	12.5 ± 4.7	8.7 ± 5.2	<0.001
Vascular risk factors, *n* (%)				
Hypertension	73 (62.4)	19 (42.2)	54 (75.0)	<0.001
Diabetes	24 (20.5)	6 (13.3)	18 (25.0)	0.128
Dyslipidaemia	34 (29.1)	9 (20.0)	25 (34.7)	0.088
Stroke	14 (12.0)	2 (4.4)	12 (16.7)	0.048
***APOE* genotyping, *n* (%)**				
APOE4 carrier	37 (32.2)	18 (41.9)	19 (26.4)	0.086
Imaging markers				
PiB positive (SUVR > 1.5)	49 (41.9%)	28 (62.2%)	21 (29.2%)	<0.001
PiB SUVR	1.62 ± 0.48	1.86 ± 0.52	1.47 ± 0.38	<0.001
Number of lacunes	4.48 ± 6.64	0.76 ± 2.22	6.75 ± 7.39	<0.001
General cognition				
CDR-SOB	1.4 ± 0.94	1.7 ± 1.1	1.3 ± 0.8	0.010
MMSE	26.1 ± 2.7	25.8 ± 2.4	26.3 ± 2.9	0.407

MMSE = Mini-Mental State Examination.

Table 2 Hazard ratios of dementia conversion

	Model 1		Model 2	
	HR (95% CI)	*P*	HR (95% CI)	*P*
Age	1.08 (1.02–1.14)	0.013	1.04 (0.97–1.11)	0.267
Gender (Ref: male)	1.87 (0.77–4.54)	0.164	2.90 (1.15–7.33)	0.024
Education	1.04 (0.95–1.14)	0.379	1.06 (0.96–1.17)	0.275
MCI subtype (Ref: amnestic MCI)	0.48 (0.19–1.19)	0.112	0.36 (0.15–0.87)	0.023
Baseline lacune number	0.99 (0.91–1.08)	0.898	0.97 (0.89–1.06)	0.494
Baseline PiB SUVR	5.29 (2.29–12.23)	<0.001	6.30 (2.59–15.33)	<0.001
Baseline nodal efficiency			<0.01 (<0.01–10.54)	0.105
Baseline cortical thickness			0.02 (<0.01–0.50)	0.016

Model 1: age, gender, education, MCI subtypes, baseline lacune number, and baseline PiB SUVR were entered as predictors.
Model 2: baseline nodal efficiency and baseline cortical thickness were entered in addition to Model 1.
HR = hazard ratio.

delayed recall (β = −0.11, SE = 0.28, *P* = 0.704), digit span backward (β = 0.03, SE = 0.05, *P* = 0.484), COWAT phonemic (β = −0.53, SE = 0.47, *P* = 0.266), or Stroop colour reading test scores (β = −1.36, SE = 1.17, *P* = 0. 245).

To investigate the effects of total CSVD score on cognitive decline, we performed linear mixed effect regression models adding time-varying CSVD scores to Model 1 instead of time-varying lacunes. However, there were no correlations between time-varying CSVD scores and cognitive decline in any domain (Supplementary Table 2).

When we incorporated time-varying regional nodal efficiency or cortical thickness parameter into Model 1, time-varying regional nodal efficiency and cortical thickness showed a negative correlation with corresponding cognitive decline: time-varying global cortical thickness for CDR-SOB; time-varying temporoparietal nodal efficiency and cortical thickness for RCFT delayed recall score; time-varying temporoparietal cortical thickness for SVLT delayed recall score; time-varying frontal nodal efficiency and time-varying frontal cortical thickness for digit span backward score; as well as time-varying frontal thickness for COWAT phonemic and Stroop colour reading test scores. Furthermore, even after adding time-varying regional nodal efficiency or cortical thickness parameters to Model 1, the association of PiB SUVR or lacune number with cognitive decline remained significant (Table 4, Models 2 and 3).

Relative impact of multimodal imaging markers on cognitive decline

Time-varying PiB SUVR (standardized β = 0.31, SE = 0.09) and cortical thickness (standardized β = −0.30, SE = 0.09)

Downloaded from https://academic.oup.com/brain/article/139/9/2516/1744564 by Hanyang Univ Lib user on 03 September 2021

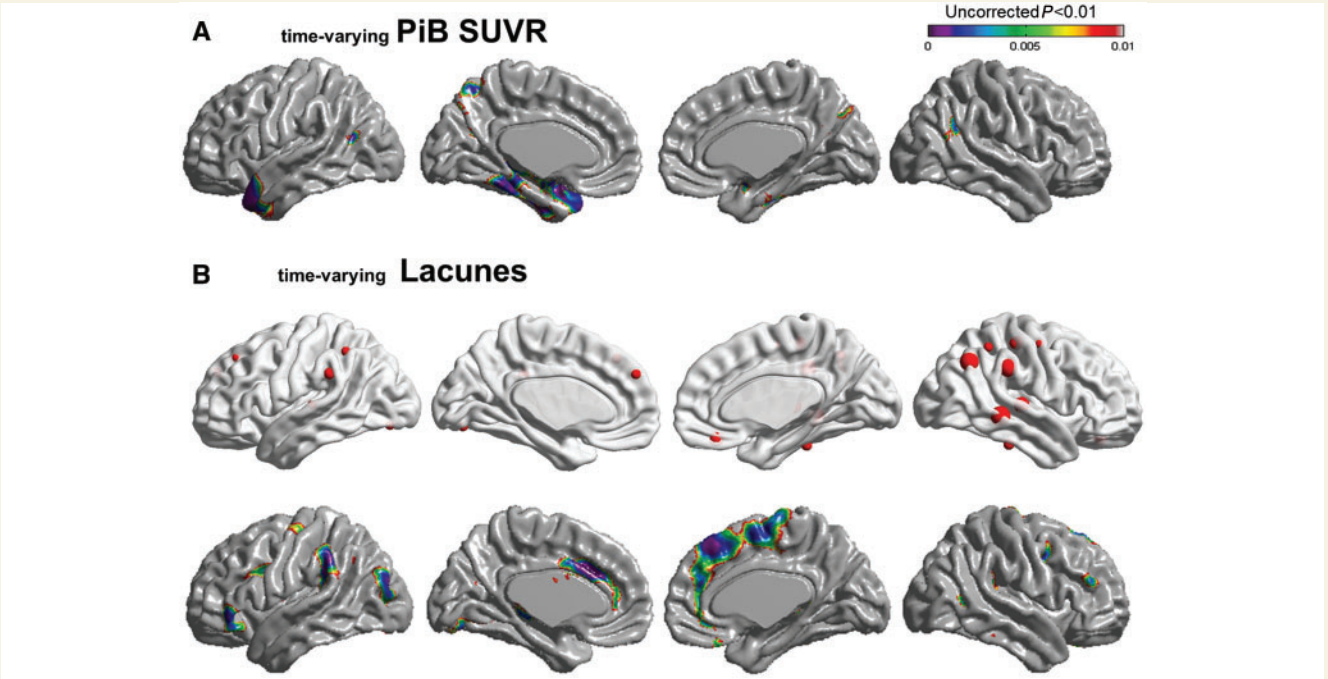

Figure 1 Brain structural changes. Figure shows changes related to longitudinal measurements of PiB SUVR (**A**) and the number of lacunes (**B**). Coloured areas represent significant cortical thinning regions and red circles indicate nodes that are significantly decreased in nodal efficiency (uncorrected $P < 0.01$). The size of the node sphere represents degree of significance. Age, gender, time interval from baseline (years), MCI subtypes, time-varying PiB SUVR, and time-varying lacune number were entered as fixed effects and subject was entered as a random effect.

Table 3 Regions with lacune-associated changes in nodal efficiency

Region	T-value	*P*-value
Right middle temporal gyrus	−3.172	<0.001
Right angular gyrus	−3.133	0.001
Right supramarginal gyrus	−3.109	0.001
Right superior temporal gyrus	−2.934	0.002
Right rectus gyrus	−2.899	0.002
Right postcentral gyrus	−2.815	0.003
Left supramarginal gyrus	−2.621	0.005
Right inferior temporal gyrus	−2.557	0.006
Right precuneus	−2.548	0.006
Left superior frontal gyrus, medial	−2.504	0.007
Left superior frontal gyrus, dorsolateral	−2.474	0.007
Right precentral gyrus	−2.430	0.008
Left inferior occipital gyrus	−2.421	0.008
Left inferior parietal lobule	−2.409	0.008
Right inferior parietal lobule	−2.394	0.009
Left superior temporal gyrus	−2.354	0.010

both showed similar effects on time-varying CDR-SOB. Time-varying PiB SUVR (standardized $\beta = -0.25$, SE = 0.09) showed the strongest effect on time-varying RCFT delayed recall score, followed by time-varying temporoparietal thickness (standardized $\beta = 0.21$, SE = 0.08) and time-varying nodal efficiency (standardized $\beta = 0.17$, SE = 0.07). Time-varying lacune number (standardized $\beta = -0.25$, SE = 0.10) showed the strongest effect on time-varying digit span backward test scores followed by time-varying nodal efficiency (standardized $\beta = 0.17$, SE = 0.08). Finally, time-varying lacune number ($\beta = -0.22$, SE = 0.10) showed the strongest effect on time-varying Stroop colour test score followed by time-varying frontal thickness (standardized $\beta = 0.19$, SE = 0.08) (Table 5).

Discussion

In this study, we assessed the relative impact of amyloid-β, lacunes and their associated downstream imaging markers on cognitive trajectories over 3 years in an MCI cohort. The major findings of our study were as follows. First, lacune progression affected structural network disruption and cortical thinning in the frontal and/or parietal areas, while amyloid-β progression affected only cortical thinning in the medial temporal and precuneus areas. Second, lacune progression affected frontal-executive function decline while amyloid-β progression affected memory decline. Furthermore, regional structural network disruption or cortical thinning contributed to corresponding cognitive decline. Finally, among the multiple imaging markers that significantly affected cognitive decline, progression of amyloid-β and lacunes were the most important imaging

Downloaded from https://academic.oup.com/brain/article/139/9/2516/1744564 by Hanyang Univ Lib user on 03 September 2021

Table 4 Mixed effects models analysing the relationship between longitudinal image marker measurements and rate of cognitive decline

	General cognition		Memory				Frontal executive					
	CDR-SOB		SVLT delayed recall		RCFT delayed recall		Digit span backward		COWAT, phonemic		Stroop colour	
	β* (SE)	*P*	β* (SE)	*P*	β* (SE)	*P*	β* (SE)	*P*	β* (SE)	*P*	β* (SE)	*P*
Model 1												
tv. Lacune	0.01 (0.01)	0.143	−0.02 (0.01)	0.165	−0.01 (0.08)	0.932	−0.05 (0.01)	0.002†	−0.01 (0.14)	0.941	−0.94 (0.35)	0.008†
tv. PiB SUVR	0.34 (0.08)	<0.001	−0.79 (0.19)	<0.001†	−2.84 (1.08)	0.009†	0.07 (0.18)	0.711	2.39 (1.76)	0.178	−0.97 (4.59)	0.833
Model 2												
tv. Lacune	0.02 (0.02)	0.378	−0.05 (0.04)	0.179	0.04 (0.08)	0.641	−0.04 (0.01)	0.008†	0.03 (0.13)	0.848	−0.88 (0.35)	0.014†
tv. PiB SUVR	0.96 (0.27)	0.001	−1.75 (0.53)	0.001†	−2.75 (1.07)	0.012†	0.01 (0.18)	0.946	2.38 (1.78)	0.184	−2.33 (4.69)	0.620
tv. Total nodal efficiency	−6.62 (3.62)	0.069										
tv. Temporoparietal nodal efficiency			2.29 (3.38)	0.500	16.67 (7.24)	0.023†						
tv. Frontal nodal efficiency							4.77 (1.92)	0.014†	40.65 (17.74)	0.023	62.58 (43.64)	0.153
Model 3												
tv. Lacune	0.02 (0.02)	0.295	−0.05 (0.04)	0.201	0.00 (0.08)	0.979	−0.04 (0.01)	0.003†	−0.02 (0.13)	0.875	−0.88 (0.34)	0.012†
tv. PiB SUVR	0.81 (0.27)	0.003	−1.57 (0.52)	0.003†	−2.34 (1.10)	0.035	0.15 (0.18)	0.430	3.58 (1.75)	0.042	0.55 (4.60)	0.905
tv. Total cortical thickness	−3.03 (0.81)	<0.001										
tv. Temporoparietal cortical thickness			3.44 (1.35)	0.012†	8.14 (2.86)	0.005†						
tv. Frontal cortical thickness							1.48 (0.51)	0.004†	15.46 (4.78)	0.002†	33.87 (11.68)	0.004†

*Unstandardized coefficient.

†$P < 0.05$ after Bonferroni correction for multiple tests (two outcomes in memory domain and three outcomes in frontal-executive domain).

SVLT = Seoul verbal learning test; RCFT = Rey complex figure test; tv. = time-varying.

Model 1: age, gender, MCI subtypes, time interval from baseline (years), time-varying number of lacunes, and time-varying PiB SUVR were entered as fixed effects; and subject was entered as a random effect.

Model 2: time-varying nodal efficiency and time-varying cortical thickness were entered as fixed effects in addition to Model 1.

Downloaded from https://academic.oup.com/brain/article/139/9/2516/1744564 by Hanyang Univ Lib user on 03 September 2021

Table 5 Relative impact of multimodal imaging markers on cognitive decline

	General cognition		Memory		Frontal-Executive			
	CDR-SOB		RCFT delayed recall		Digit span backward		Stroop colour	
	β* (SE)	*P*	β* (SE)	*P*	β* (SE)	*P*	β* (SE)	*P*
tv. Lacune	−0.01 (0.10)	0.615	0.07 (0.10)	0.488	−0.25 (0.10)	0.014†	−0.22 (0.10)	0.034
tv. PiB SUVR	0.31 (0.09)	0.001	−0.25 (0.09)	0.010	0.02 (0.10)	0.827	−0.04 (0.10)	0.697
tv. Total nodal efficiency	−0.06 (0.09)	0.385						
tv. Total cortical thickness	−0.30 (0.09)	<0.001						
tv. Temporoparietal nodal efficiency			0.17 (0.07)	0.024				
tv. Temporoparietal cortical thickness			0.21 (0.08)	0.010				
tv. Frontal nodal efficiency					0.17 (0.08)	0.021†	0.07 (0.07)	0.348
tv. Frontal cortical thickness					0.13 (0.08)	0.121	0.19 (0.08)	0.026

*Standardized coefficient.
†$P < 0.05$ after Bonferroni correction for multiple tests (two outcomes in frontal-executive domain).
RCFT = Rey complex figure test; tv. = time-varying.

markers associated with decline in memory and frontal-executive function, respectively. Considered as a whole, our findings suggest that amyloid-β and lacunes have distinctive effects on downstream imaging trajectories and cognitive trajectories. In addition, amyloid-β and lacunes each had the greatest contribution on corresponding cognitive decline, even when taking into account the effect of their downstream imaging markers.

Our first major finding was that progression of amyloid-β and lacunes distinctively affected their downstream imaging trajectories. Specifically, lacune progression was associated with cortical thinning in the frontal and parietal regions, sparing the medial temporal and precuneus regions, while amyloid-β progression was associated with cortical thinning in the medial temporal and precuneus regions. Consistent with previous cross-sectional studies (Ye *et al.*, 2015), sparing of these regions may therefore be a feature discriminating the effects of CSVD from those of amyloid-β progression. CSVD progression was also associated with structural network disruption in the frontal and parietal regions, sparing the medial temporal and precuneus regions. This finding corroborates the notion that ischaemia specifically affects white matter in frontal and parietal regions rather than in temporal and occipital regions (Moody *et al.*, 1990; Gootjes *et al.*, 2004; Wen and Sachdev, 2004). This suggests that the progression of amyloid-β and lacunes distinctively affect their downstream imaging trajectories in terms of related topography and the type of downstream imaging marker.

Our second major finding, that progression of amyloid-β and lacunes affected distinctive cognitive trajectories was supported by the following observations. First, the progression of lacunes affected decline in frontal-executive function while amyloid-β progression affected memory decline. Second, downstream imaging trajectories related to amyloid-β and lacune progression also contributed to corresponding cognitive decline. These findings are in line with previous longitudinal studies showing that memory decline is related to amyloid-β and hippocampal atrophy, whereas frontal-executive function decline is more associated with lacunes (Mungas *et al.*, 2005; Mattsson *et al.*, 2015). Our results are also consistent with previous cross-sectional studies showing that amyloid-β and lacune burden affects impairments in specific cognitive domains with the mediation of region-specific structural networks and/or cortical atrophy (Ye *et al.*, 2015). Therefore, it may be the case that cerebral hypoperfusion induced by lacunes can cause white matter network disruption, which in turn leads to secondary damage to neuronal cell bodies and grey matter atrophy in the frontal region, eventually resulting in frontal-executive function decline. On the other hand, amyloid-β burden may affect cortical thinning through several mechanisms, including cascades of tau pathology, hypometabolism, or functional network disruption rather than structural network disruption, resulting in memory decline. Interestingly, the association between amyloid-β or lacune progression and corresponding cognitive decline remained significant even after controlling for structural network disruption and cortical thinning.

The last major finding of our study was that amyloid-β and lacune progression contributed to cognitive decline to an extent greater than or at least similar to their downstream changes. That is, the effects of amyloid-β or lacunes on cognition were only partially mediated by structural network disruption or cortical thinning, leaving a large proportion of their effects as direct or mediated by other possible routes. There are several possible explanations. Amyloid-β or lacunes may directly disconnect synapses or reduce neurotransmitter concentrations to an extent that affects cognition but does not change brain structure. Alternatively, amyloid-β or lacune progression might affect cognitive decline through mechanisms that were not quantified in this study, such as subcortical structures or functional networks (Reijmer *et al.*, 2013; Kim *et al.*, 2015*a*). Indeed, a cross-sectional study of non-demented elderly patients showed that temporal amyloid-β deposition contributed to memory impairment independent of hippocampal atrophy (Chetelat *et al.*, 2011), and a longitudinal

Downloaded from https://academic.oup.com/brain/article/139/9/2516/1744564 by Hanyang Univ Lib user on 03 September 2021

study showed that amyloid-β is strongly associated with memory decline, independent of brain structural or functional changes (Mattsson *et al.*, 2015). The present study showed that although multiple imaging markers such as amyloid-β, lacunes, structural network, and cortical thickness all independently contribute to cognitive decline, amyloid-β had the greatest impact on memory decline and lacunes had the greatest impact on frontal-executive decline.

We found that both amyloid-β and lacunes progressed over time, but the progression rates were negatively correlated (subjects with higher amyloid-β progression exhibited less lacune progression). Several cross-sectional studies have shown inconsistent results regarding the relationship between amyloid-β and lacunes. Some studies have shown a positive correlation (Grimmer *et al.*, 2012; Noh *et al.*, 2014) while other studies have shown an absence of (Marchant *et al.*, 2012) or negative correlation (Provenzano *et al.*, 2013; Lee *et al.*, 2014). However, to our knowledge, there have been no longitudinal studies conducted that have evaluated the relationship between amyloid-β and lacune progression. The negative correlation between amyloid and lacunes might have resulted from 'index event bias'. That is, as both lacunes and amyloid burden causes cognitive impairments, subcortical vascular MCI patients who all have severe lacunes need less amyloid burden than amnestic MCI patients with mild lacunes, to reach certain level of cognitive impairment. However, it is less likely because our study was designed as a longitudinal study. Another possible explanation for the negative correlation between amyloid-β and lacune progression in this study might be that lacune progression affects cortical thinning, which in turn decreases the cortical regions for amyloid-β deposition.

We could not find evidence for an interactive effect of amyloid-β and lacunes on cognitive decline. An interrelationship has been suggested between amyloid-β and CSVD, as results from preclinical studies support the hypothesis that abnormal vessels interrupt amyloid-β clearance (Lee *et al.*, 2011*b*; Li *et al.*, 2014). Additionally, a previous cross-sectional study raised the possibility that amyloid-β and CSVD might synergistically affect cognitive impairment (Lee *et al.*, 2014). However, a human imaging study has suggested that amyloid-β and CSVD are poorly correlated, and a more recent longitudinal study showed that amyloid-β and CSVD are independent in their relationship with cognitive decline (Park *et al.*, 2014; Vemuri *et al.*, 2015). It seems plausible that the stage of disease severity matters when evaluating interactions between biomarkers. It may also be possible that during the lifelong accumulation of amyloid-β and vascular related factors, one may have influenced another. Further studies with a larger sample size and longer follow-up duration are needed for more definitive conclusions.

The strengths of our study are that we prospectively recruited patients who were on the amyloid-β pathway and those who were on the vascular pathway, and that we have combined repeatedly measured multimodal imaging markers into analyses. However, there are several limitations. First of all, we did not measure WMH volume longitudinally due to high variability in the WMH measurements. Second, we could not consider the effects of other pathologies including other Alzheimer's disease (soluble amyloid-β and neurofibrillary tangles), microinfarcts or possible combined degenerative dementia (dementia with Lewy bodies and frontotemporal dementia) pathologies, which are also associated with cognitive impairments. Third, we were not able to capture physiological or biochemical downstream events triggered by amyloid-β or lacunes. Further studies on the role of synaptic dysfunction, inflammation, and oxidative stress on cognitive function and their relationship to amyloid-β/lacunes are needed. In addition, the sample size and follow-up duration might not be sufficient to demonstrate the interactive effects of amyloid-β and lacunes. However, our results do appear to provide rationale for the targeting of amyloid-β and lacunes in new drug trials aimed at ameliorating cognitive decline. Further studies may allow for the identification of specific imaging markers that are more precisely aligned with cognitive decline.

Funding

This study was supported by grants from the Korea Healthcare Technology R&D Project, through the Korea Health Industry Development Institute (KHIDI), funded by the Ministry of Health & Welfare, Republic of Korea (HI14C2768); the Korean Science and Engineering Foundation (KOSEF) NRL program funded by the Korean government [MEST; 2011-0028333]; Korea Ministry of Environment (MOE) as the Environmental Health Action Program (2014001360002); the Korean Neurological Association (KNA-15-MI-08); and the National Research Foundation of Korea (NRF) grant funded by the Korea government (MSIP) (NRF-2015R1C1A2A01053281). All authors had full access to all the data in the study and had final responsibility for the decision to submit for publication

References

Ahn HJ, Chin J, Park A, Lee BH, Suh MK, Seo SW, et al. Seoul neuropsychological screening battery-dementia version (SNSB-D): a useful tool for assessing and monitoring cognitive impairments in dementia patients. J Korean Med Sci 2010; 25: 1071–6.

Beaulieu C. The basis of anisotropic water diffusion in the nervous system - a technical review. NMR Biomed 2002; 15: 435–55.

Chetelat G, Villemagne VL, Pike KE, Ellis KA, Bourgeat P, Jones G, et al. Independent contribution of temporal beta-amyloid deposition to memory decline in the pre-dementia phase of Alzheimer's disease. Brain 2011; 134: 798–807.

Collins DL, Neelin P, Peters TM, Evans AC. Automatic 3D intersubject registration of MR volumetric data in standardized talairach space. J Comput Assist Tomogr 1994; 18: 192–205.

Downloaded from https://academic.oup.com/brain/article/139/9/2516/1744564 by Hanyang Univ Lib user on 03 September 2021

Ewers M, Walsh C, Trojanowski JQ, Shaw LM, Petersen RC, Jack CR Jr, et al. Prediction of conversion from mild cognitive impairment to Alzheimer's disease dementia based upon biomarkers and neuropsychological test performance. Neurobiol Aging 2012; 33: 1203–14.

Fein G, Di Sclafani V, Tanabe J, Cardenas V, Weiner MW, Jagust WJ, et al. Hippocampal and cortical atrophy predict dementia in subcortical ischemic vascular disease. Neurology 2000; 55: 1626–35.

Gootjes L, Teipel SJ, Zebuhr Y, Schwarz R, Leinsinger G, Scheltens P, et al. Regional distribution of white matter hyperintensities in vascular dementia, Alzheimer's disease and healthy aging. Dement Geriatr Cogn Disord 2004; 18: 180–8.

Grimmer T, Faust M, Auer F, Alexopoulos P, Forstl H, Henriksen G, et al. White matter hyperintensities predict amyloid increase in Alzheimer's disease. Neurobiol Aging 2012; 33: 2766–73.

Jack CR, Knopman DS, Jagust WJ, Petersen RC, Weiner MW, Aisen PS, et al. Tracking pathophysiological processes in Alzheimer's disease: an updated hypothetical model of dynamic biomarkers. Lancet Neurol 2013; 12: 207–16.

Kang Y, Na DL. Seoul neuropsychological screening battery (SNSB). Hum Brain Research & Consulting Co, Incheon 2003.

Kim H, Na DL. Normative data on the Korean version of the boston naming test. J Clin Exp Neuropsychol 1999; 21: 127–33.

Kim HJ, Cha J, Lee JM, Shin JS, Jung NY, Kim YJ, et al. Distinctive resting state network disruptions among Alzheimer's disease, subcortical vascular dementia, and mixed dementia patients. J Alzheimers Dis 2016; 50: 709–18.

Kim HJ, Im K, Kwon H, Lee JM, Kim C, Kim YJ, et al. Clinical effect of white matter network disruption related to amyloid and small vessel disease. Neurology 2015a; 85: 63–70.

Kim HJ, Im K, Kwon H, Lee JM, Ye BS, Kim YJ, et al. Effects of amyloid and small vessel disease on white matter network disruption. J Alzheimers Dis 2015b; 44: 963–75.

Kim HJ, Ye BS, Yoon CW, Noh Y, Kim GH, Cho H, et al. Cortical thickness and hippocampal shape in pure vascular mild cognitive impairment and dementia of subcortical type. Eur J Neurol 2014; 21: 744–51.

Kim MJ, Seo SW, Kim GH, Kim ST, Lee JM, Qiu A, et al. Less depressive symptoms are associated with smaller hippocampus in subjective memory impairment. Arch Gerontol Geriatr 2013; 57: 110–15.

Kim SH, Seo SW, Go SM, Chin J, Lee BH, Lee JH, et al. Pyramidal and extrapyramidal scale (PEPS): a new scale for the assessment of motor impairment in vascular cognitive impairment associated with small vessel disease. Clin Neurol Neurosurg 2010; 113: 181–7.

Ku HM, Kim JH, Kwon EJ, Kim SH, Lee HS, Ko HJ, et al. A study on the reliability and validity of Seoul-instrumental activities of daily living (S-IADL). J Korean Neuropsychiatr Assoc 2004; 43: 189–99.

Lee JH, Kim SH, Kim GH, Seo SW, Park HK, Oh SJ, et al. Identification of pure subcortical vascular dementia using 11C-Pittsburgh compound B. Neurology 2011a; 77: 18–25.

Lee JS, Im DS, An YS, Hong JM, Gwag BJ, Joo IS. Chronic cerebral hypoperfusion in a mouse model of Alzheimer's disease: an additional contributing factor of cognitive impairment. Neurosci Lett 2011b; 489: 84–8.

Lee MJ, Seo SW, Na DL, Kim C, Park JH, Kim GH, et al. Synergistic effects of ischemia and beta-amyloid burden on cognitive decline in patients with subcortical vascular mild cognitive impairment. JAMA Psychiatry 2014; 71: 412–22.

Li H, Guo Q, Inoue T, Polito VA, Tabuchi K, Hammer RE, et al. Vascular and parenchymal amyloid pathology in an Alzheimer disease knock-in mouse model: interplay with cerebral blood flow. Mol Neurodegener 2014; 9: 28.

Lo RY, Jagust WJ, Initia ADN. Vascular burden and Alzheimer disease pathologic progression. Neurology 2012; 79: 1349–55.

Marchant NL, Reed BR, DeCarli CS, Madison CM, Weiner MW, Chui HC, et al. Cerebrovascular disease, beta-amyloid, and cognition in aging. Neurobiol Aging 2012; 33: 1006.

Mattsson N, Insel PS, Aisen PS, Jagust W, Mackin S, Weiner M, et al. Brain structure and function as mediators of the effects of amyloid on memory. Neurology 2015; 84: 1136–44.

Moody DM, Bell MA, Challa VR. Features of the cerebral vascular pattern that predict vulnerability to perfusion or oxygenation deficiency: an anatomic study. AJNR Am J Neuroradiol 1990; 11: 431–9.

Mori S, Crain BJ, Chacko VP, van Zijl PCM. Three-dimensional tracking of axonal projections in the brain by magnetic resonance imaging. Ann Neurol 1999; 45: 265–9.

Mungas D, Harvey D, Reed BR, Jagust WJ, DeCarli C, Beckett L, et al. Longitudinal volumetric MRI change and rate of cognitive decline. Neurology 2005; 65: 565–71.

Mungas D, Jagust WJ, Reed BR, Kramer JH, Weiner MW, Schuff N, et al. MRI predictors of cognition in subcortical ischemic vascular disease and Alzheimer's disease. Neurology 2001; 57: 2229–35.

Noh Y, Seo SW, Jeon S, Lee JM, Kim JH, Kim GH, et al. White matter hyperintensities are associated with amyloid burden in APOE4 non-carriers. J Alzheimers Dis 2014; 40: 877–86.

Park JH, Seo SW, Kim C, Kim SH, Kim GH, Kim ST, et al. Effects of cerebrovascular disease and amyloid beta burden on cognition in subjects with subcortical vascular cognitive impairment. Neurobiol Aging 2014; 35: 254–60.

Petersen RC. Mild cognitive impairment as a diagnostic entity. J Intern Med 2004; 256: 183–94.

Petersen RC, Smith GE, Waring SC, Ivnik RJ, Tangalos EG, Kokmen E. Mild cognitive impairment: clinical characterization and outcome. Arch Neurol 1999; 56: 303–8.

Preul C, Lohmann G, Hund-Georgiadis M, Guthke T, von Cramon DY. Morphometry demonstrates loss of cortical thickness in cerebral microangiopathy. J Neurol 2005; 252: 441–7.

Provenzano FA, Muraskin J, Tosto G, Narkhede A, Wasserman BT, Griffith EY, et al. White matter hyperintensities and cerebral amyloidosis necessary and sufficient for clinical expression of Alzheimer disease? JAMA Neurol 2013; 70: 455–61.

Reijmer YD, Leemans A, Caeyenberghs K, Heringa SM, Koek HL, Biessels GJ, et al. Disruption of cerebral networks and cognitive impairment in Alzheimer disease. Neurology 2013; 80: 1370–7.

Rubinov M, Sporns O. Complex network measures of brain connectivity: uses and interpretations. Neuroimage 2010; 52: 1059–69.

Sabri O, Ringelstein EB, Hellwig D, Schneider R, Schreckenberger M, Kaiser HJ, et al. Neuropsychological impairment correlates with hypoperfusion and hypometabolism but not with severity of white matter lesions on MRI in patients with cerebral microangiopathy. Stroke 1999; 30: 556–66.

Schneider JA, Arvanitakis Z, Bang W, Bennett DA. Mixed brain pathologies account for most dementia cases in community-dwelling older persons. Neurology 2007; 69: 2197–204.

Seo SW, Ahn J, Yoon U, Im K, Lee JM, Tae Kim S, et al. Cortical thinning in vascular mild cognitive impairment and vascular dementia of subcortical type. J Neuroimaging 2010; 20: 37–45.

Seo SW, Cho SS, Park A, Chin J, Na DL. Subcortical vascular versus amnestic mild cognitive impairment: comparison of cerebral glucose metabolism. J Neuroimaging 2009; 19: 213–19.

Seo SW, Im K, Lee JM, Kim YH, Kim ST, Kim SY, et al. Cortical thickness in single- versus multiple-domain amnestic mild cognitive impairment. Neuroimage 2007; 36: 289–97.

Seo SW, Lee JM, Im K, Park JS, Kim SH, Kim ST, et al. Cortical thinning related to periventricular and deep white matter hyperintensities. Neurobiol Aging 2012; 33: 1156–67.

Staals J, Makin SD, Doubal FN, Dennis MS, Wardlaw JM. Stroke subtype, vascular risk factors, and total MRI brain small-vessel disease burden. Neurology 2014; 83: 1228–34.

Tzourio-Mazoyer N, Landeau B, Papathanassiou D, Crivello F, Etard O, Delcroix N, et al. Automated anatomical labeling of activations in SPM using a macroscopic anatomical parcellation of the MNI MRI single-subject brain. Neuroimage 2002; 15: 273–89.

Downloaded from https://academic.oup.com/brain/article/139/9/2516/1744564 by Hanyang Univ Lib user on 03 September 2021

Vemuri P, Lesnick TG, Przybelski SA, Knopman DS, Preboske GM, Kantarci K, et al. Vascular and amyloid pathologies are independent predictors of cognitive decline in normal elderly. Brain 2015; 138: 761–71.

Villeneuve S, Reed BR, Wirth M, Haase CM, Madison CM, Ayakta N, et al. Cortical thickness mediates the effect of beta-amyloid on episodic memory. Neurology 2014; 82: 761–7.

Wang R, Beener T, Sorensen AG, Wedeen VJ. Diffusion toolkit: a software package for diffusion imaging data processing and tractography. Proc Int Soc Magn Reson Med 2007; 15: 3720.

Wardlaw JM, Smith EE, Biessels GJ, Cordonnier C, Fazekas F, Frayne R, et al. Neuroimaging standards for research into small vessel disease and its contribution to ageing and neurodegeneration. Lancet Neurol 2013; 12: 822–38.

Wen W, Sachdev PS. Extent and distribution of white matter hyperintensities in stroke patients: the Sydney stroke study. Stroke 2004; 35: 2813–19.

Ye BS, Seo SW, Kim GH, Noh Y, Cho H, Yoon CW, et al. Amyloid burden, cerebrovascular disease, brain atrophy, and cognition in cognitively impaired patients. Alzheimers Dement 2015; 11: 496–503.

Downloaded from https://academic.oup.com/brain/article/139/9/2516/1744564 by Hanyang Univ Lib user on 03 September 2021